J Mater Sci (2023) 58:1680–1693

Electronic materials

Wearable humidity sensor embroidered on a commercial face mask and its electrical properties

Ankita Sinha[1,*], Adrian K. Stavrakis[1], Mitar Simić[1], and Goran M. Stojanović[1]

[1] University of Novi Sad, Faculty of Technical Sciences, Trg Dositeja Obradovića 6, Novi Sad 21000, Serbia

Received: 22 September 2022
Accepted: 29 December 2022
Published online: 11 January 2023

ABSTRACT

Owing to the rapid development in the field of e-textile-based flexible and portable sensors, the present work demonstrates a fully textile-based stretchable face mask humidity sensor which was created using digital embroidery technique. The design of the sensor was comprised of interdigitated structured electrodes made up of polymer core-based conductive silver-coated threads and hygroscopic threads embedded between them. The fabricated sensor performed well towards moisture detection in accordance with the principle where resistance of the face mask sensor decreased with the increase in the relative humidity along with the changing operational frequency in the range from 1 Hz to 200 kHz. The electrical response (resistance, impedance, capacitance and phase angle) of the novel thread-based sensor towards change in relative humidity was recorded and showed in the present work. The embroidery of polymer-based threads onto the face mask towards humidity sensing offers a novel wearable platform for more extended biomedical applications for detection of various breath biomarkers and thus early diagnosis of diseases.

Introduction

With numerous applications in the field of agriculture, medicine and other industries, humidity sensors have drawn considerable attraction in recent times. One of their significant roles includes noninvasive monitoring of breathing to evaluate human health as water vapor is a dominant part (> 90%) in the exhaled breath [1]. Numerous efforts have been made in the past years to investigate various transduction mechanisms to develop humidity sensors including capacitive, resistive, surface acoustic and optical-based [1, 2]. A variety of nanomaterials such as carbon allotropes, metal nanoparticles and nanocomposites have been used as humidity-sensitive materials [3]; however, demands for flexible materials have been raised in recent times for developing high-performance humidity sensors [4, 5]. Various polymer materials such as poly(dimethylsiloxane)

Handling Editor: David Cann.

Address correspondence to E-mail: ankitasinha11@outlook.com

https://doi.org/10.1007/s10853-022-08135-2

(PDMS) [6], poly(ethylene terephthalate) (PET) [7] and poly(ethylene naphthalate) (PEN) [8] have been applied as thin films to fabricate wearable humidity sensors; however, they have limited hygroscopicity and breathability, which reduces their sensitivity and comfort. Moreover, paper-based sensors demonstrate high fragility [9]. The impressive development in the field of e-textiles (including natural, e.g., cotton and silk, and synthetic, e.g., polymer-based) has caused a surge in the fabrication of textile-based humidity sensors owing to their specific fibers and voids, flexibility, durability, hygroscopic nature, breathability and wearing comfort [5, 10–12].

Wearing face mask is a form of personal protection that can minimize the inhalation of airborne particles and reduce the spread of viral and bacterial contamination, especially during the time of COVID-19 pandemic. Recent reports suggest decontamination methods of face mask and other personal protection equipments where pathogens can be effectively inactivated by temperature and moist humidity [13]. Taking inspiration from this, we present a wearable humidity sensor prototype consisting of conductive interdigitated electrodes (IDE) and moisture-sensitive hygroscopic threads embroidered on face mask capable of detecting the change in relative humidity (RH) which can further be taken into consideration to prevent viral or other pathogen infections. COVID-19 is more likely to be a sign of coughing and sneezing during which the humidity around our mouth and nose becomes relatively high making it crucial to significantly monitor the humidity around that area. The present work considers this need and exploits the face mask prototype for humidity sensing application.

Fabrication of sensors through modern embroidery technique provides numerous benefits including stretchability of sensors, high throughput and rapid manufacturing with great functionality, which are compatible for flexible electronics. Furthermore, embroidery offers an opportunity to integrate electrode patterns made up of threads into substrate to fabricate various kinds of sensors, majority of which can be utilized for biomedical applications [14, 15]. The technique allows flexibility with respect to selecting a wide range of electrode, sensing/substrate materials and sensor design. Recently, design of IDE arrays has withdrawn considerable attention, which are microelectrodes onto a suitable substrate having the appearance of interlaced fingers separated, by a gap of small distance with a number of promising advantages such as avoiding the need for a reference electrode and providing quick reaction kinetics [16, 17]. The IDE have been widely investigated to optimize the electrode gap size, electrode height using various materials, for example, silver, gold, palladium, indium tin oxide and substrates such as ceramic, glass and flexible plastics. Most frequently used RH sensors fall under mainly two categories capacitive and resistive. In capacitive sensors, the sensing layer acts as the dielectric between two parallel interdigitated electrodes [18] while in resistive sensors, the sensing layer acts as a resistor between two electrodes in an interdigitated pattern [16]. As a result, the reaction of a capacitive sensor to humidity change is measured by a change in the capacitance of the sensor while by a change in resistance of the sensor for a resistive sensor. The literature reports that silver-based IDE structures have been fabricated frequently in the past to perform humidity analysis due to their high conductivity, however, mostly by using silver ink which are highly toxic [19–21].

Herein, we present a thread-based humidity sensor prototype embroidered on a commercial single-use polypropylene face mask where the IDE structures were stitched using silver-plated polyamide threads and the moisture-sensitive thread is composed of polyester (Scheme 1a). The advantages of using polymer-based threads in humidity sensing lie in the fact that polymer groups possess different surface morphologies, several polar groups such as NR_3^+Cl, SO_3H, COOH and CO [22] and composed essentially in the form of long porous nanofibrous filaments which help in the interaction between water molecules and hygroscopic groups and results in the easy transmission of water. A short overview of the previously reported textile-based humidity sensors is provided in Table 1 where the comparison of the present sensor has been established. The sensing properties of the presented sensor were investigated over a wide range of 30–79% RH. The possible humidity sensing mechanism (Scheme 1b) of the sensor has been discussed in detail upon absorption of water molecules by hygroscopic thread, thereby generating different levels of RH. While extensive reports on sensitive materials for capacitance change has been reported toward humidity sensing, the presented textile-based sensor prototype was able to mark changes in electrical resistance of the sensor manifesting a unique humidity-sensing platform for real-time applications. Altogether, a hitherto

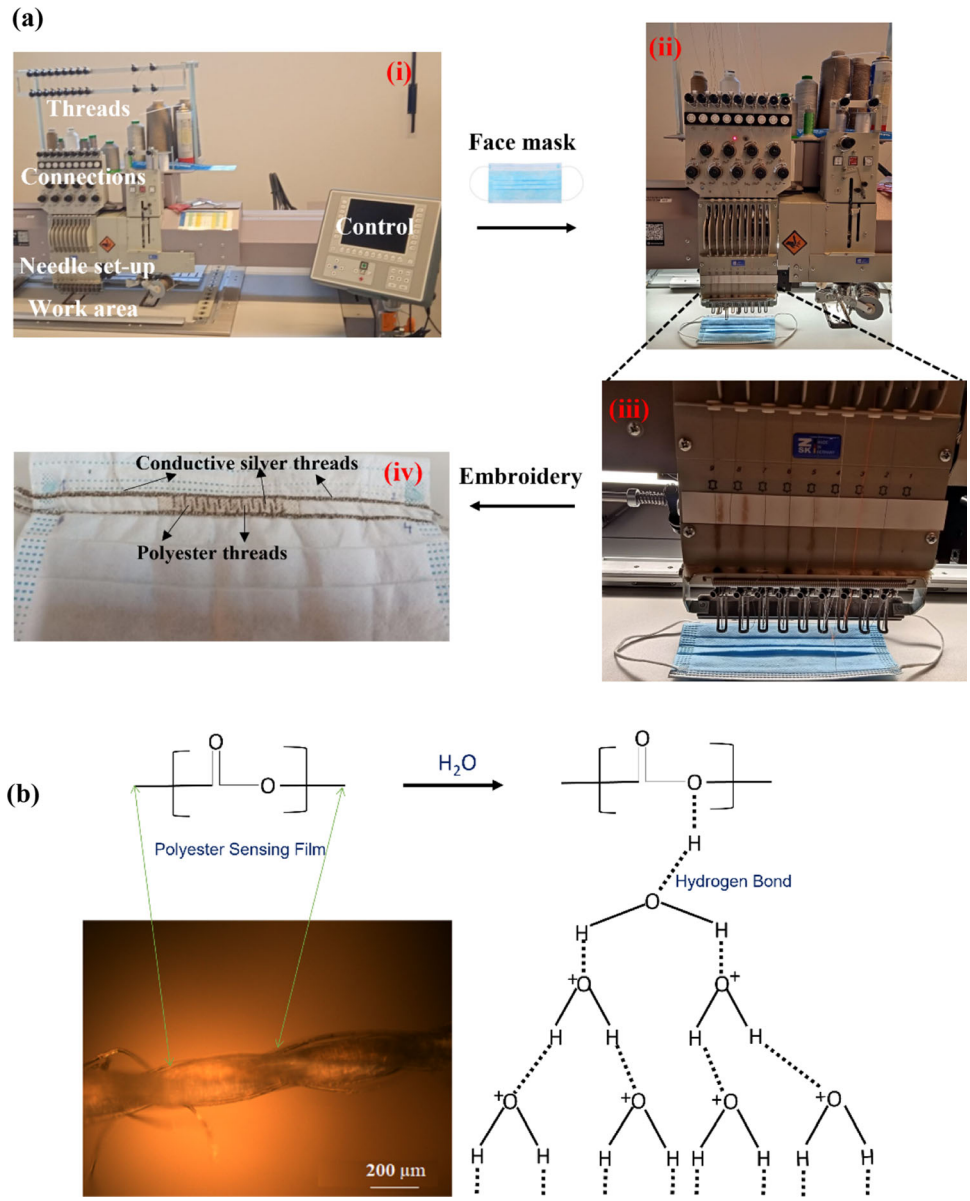

Scheme 1 (**a**) Preparation of the face mask sensor (i) rough layout of the commercial embroidery machine, (ii) placement of the face mask in the work area, (iii) enlarged view of the needle setup and work area, (iv) embroidered face mask with IDEs and moisture-sensitive polyester threads; (**b**) proposed moisture sensing mechanism at hygroscopic polyester threads (optical image) within embroidered face mask.

uninvestigated application of a thread-based humidity sensor has been taken into consideration manifesting high sensitivity towards resistance change with the increase in relative humidity which has also been compared to changes in capacitance, impedance and phase angle.

Experimental

Materials and instruments

The humidity sensor was fabricated on a single-use nonwoven polypropylene face mask purchased from a local pharmacy. The IDE were embroidered using a polyamide core-based silver-plated conductive thread (Silver-Tech 150) supplied by AMANN. The fingers between the interdigitated electrodes were filled using moisture-sensitive polyester thread (Burmilon #200 weight) by Madeira which acted as hygroscopic material. The design of the sensor was created in AutoCAD 2021 (Autodesk, USA) and embroidered using an industrial technical embroidery machine (JCZA 0109-550, ZSK Germany). The humidity measurements were taken in Owlstone system (V-OVG, Owlstone Ltd Cambridge UK) electrically connected to a chemical impedance analyzer (IM3590, Hioki, Japan) to record the electrical

Table 1 Textile-based humidity/respiration sensors

Substrate	IDE material	Sensing layer	Fabrication method	Detection range (RH)	Sensor type	Application	References
Cotton, linen	Silver-coated polymer kuraray	MIL-96(Al) Metal organic framework (MOF)	Hand stitching (IDE) and Langmuir–Blodgett film deposition (sensing layer)	3.7–90%	Capacitive	Volatile organic compound detection (VOCs)	[5]
Nonwoven cotton	Chromium–gold	Graphene oxide (GO)	Magnetron sputtering (IDE) and chemical modification with bovine serum albumin (sensing layer)	44–91%	Resistive	Respiration monitoring	[10]
Silk	Nickel	GO	Electroless plating (IDE) and spray coating (sensing layer)	–	Electrochemical	Respiration monitoring	[11]
Polyimide/textile	Silver	Nafion-based	Inkjet printing (IDE) and micropipetting (sensing layer)	5–95%	Resistive	–	[12]
Nonwoven polypropylene	Silver-coated polyamide	Polyester	Embroidery (IDE and sensing layer)	28–78%, 36–74%	Capacitive	Respiration monitoring	[18]
Nonwoven polypropylene	Silver-coated polyamide	Polyester	Embroidery (IDE and sensing layer)	30–79%	Resistive	Respiration monitoring	Present work

parameters change with variation of relative humidity, in the frequency range from 1 Hz to 200 kHz. Scanning electron microscopy (SEM) of threads were taken using TM3030, Hitachi, Japan, at an accelerating voltage of 10 kV. Energy-dispersive X-ray (EDX) and mapping analysis were performed using Bruker Quantax 70, equipped with ESPRIT compact software. Optical images were taken using Huvitz microscope with Panasis software. Manual probe station (SUSS PM5) with Motic images plus 3.0 software was used for capturing images of prepared sensor.

Experimental setup

The humidity testing was performed in a sealed glass bottle chamber where the embroidered face mask sensor comprising of IDEs and the embedded moisture-sensitive hygroscopic threads was exposed to water, at a constant temperature of 25 °C. The conductive thread-based embroidered electrodes of the face mask sensor were attached with two wires to the test setup which led to the impedance analyzer. Different levels of RH were generated in the range from 30 to 79% by a manually controlled input and output wet airflow system equipped with a humidity sensing apparatus to record the sensitivity of the face mask sensor during which water vapors were adsorbed by the textile threads. All the measurements were taken in normal laboratory conditions. The overall design of the embroidered face mask sensor is shown in Fig. 1a, b. The experimental setup comprising of humidity chamber connected to the Owlstone testing instrument is presented in Fig. 1c, while captured magnified image of our designed sensor is depicted in Fig. 1d. SEM images of conductive silver thread and polyester threads with long filament morphology are shown in Fig. 2a, b. The presence of silver particles is clearly shown in Fig. 2a which was confirmed by EDX measurement (Fig. 2c) while the presence of carbon (C) and oxygen (O) justifies the water absorbing group (C=O) of polyester threads (Fig. 2d) [18]. Moreover, elemental mapping of conductive silver thread and polyester thread is shown in Figure S1 and Figure S2 of Supplementary Information (SI).

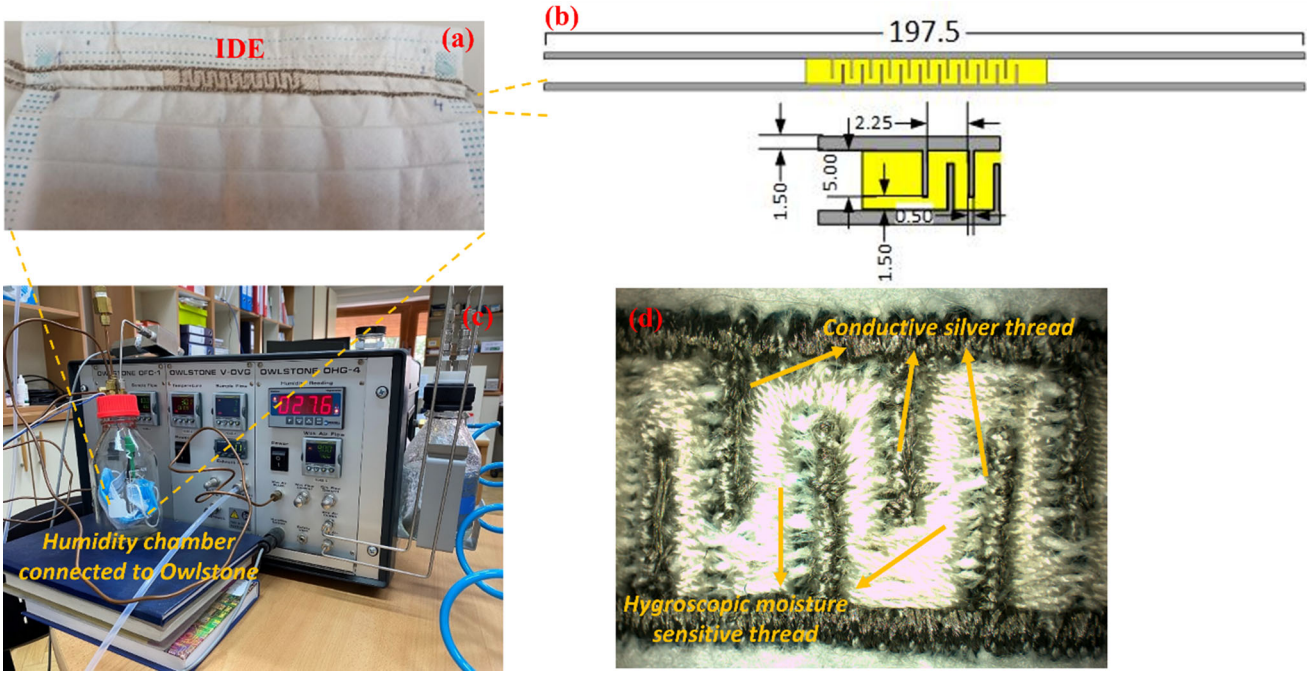

Figure 1 (**a**) Face mask sensor for humidity detection; (**b**) sensor design comprising of IDE (in gray color) and filled embedded hydroscopic threads between them (in yellow color), the dimensions are shown in mm; (**c**) humidity chamber connected to the Owlstone humidity generating machine; (**d**) captured image of face mask sensor.

Results and discussion

Humidity sensing mechanism

Unlike capacitive sensors where a sensing material with very low conductivity is required for effective use as a dielectric material [18], resistive sensors rely upon the flow of current through the sensing layer [16, 23]. Therefore, as the sensing layer (in this work polyester threads) react to the presence of water, the conductivity of the hygroscopic thread changes. In other words, as the thread-based sensor is exposed to different RH levels, it consequently leads to a change in the resistance of the sensor. In the present case, the resistive IDEs represent a chain of individual resistors arranged in parallel. The polyester core-based moisture-sensitive threads embroidered between the fingers of IDE served as water adsorption centers to create the Van der Waals interactions between the carbonyl group (C=O) of the polymer [18] and water molecules [22]. The hydrogen bonds that formed as shown in Scheme 1b play a dominant role in eliciting the sensor response [24]. In principle, C=O groups and the weak hydrogen bonds offer synergistically the unique physicochemical and electronic properties for humidity sensing to the sensor [25]. Initially, the chemisorbed water molecules are formed followed by the physical adsorption of water vapors onto the chemisorbed layer of the moisture-sensitive threads as relative humidity levels increase. Moreover, H_3O^+ formed during the adsorption of water generates charge carriers caused by the ionization of water molecules under an electrostatic field [26]. At lower humidity levels, the ion transfer is relatively difficult to achieve as very few water molecules are absorbed at sensor surface. Hence, water absorption is not continuous and thus coverage of water on the film surface [27]. However, at higher humidity levels, the multilayer physisorption of water molecules shows a more liquid-like behavior and transfer of H^+ ions (proton hopping) can be realized as $H_2O + H_3O^{+-} = H_3O^+ + H_2O$ throughout the sensing layer caused by the Grotthuss chain reaction [27]. In simple words, it can be said that H^+ ions could transfer between adjacent water molecules. Therefore, at high-humidity conditions, more water molecules are available to penetrate the interlayers of sensitive threads, which are ionized to form hydronium ions H_3O^+, which also act as dominant charge carriers. Such conditions lead to a great decrease in sensor resistance, or simply in other words, transfer of H^+ or H_3O^+ ions within moisture-sensitive threads causes a swift decrease in resistance making the sensor highly sensitive to humidity.

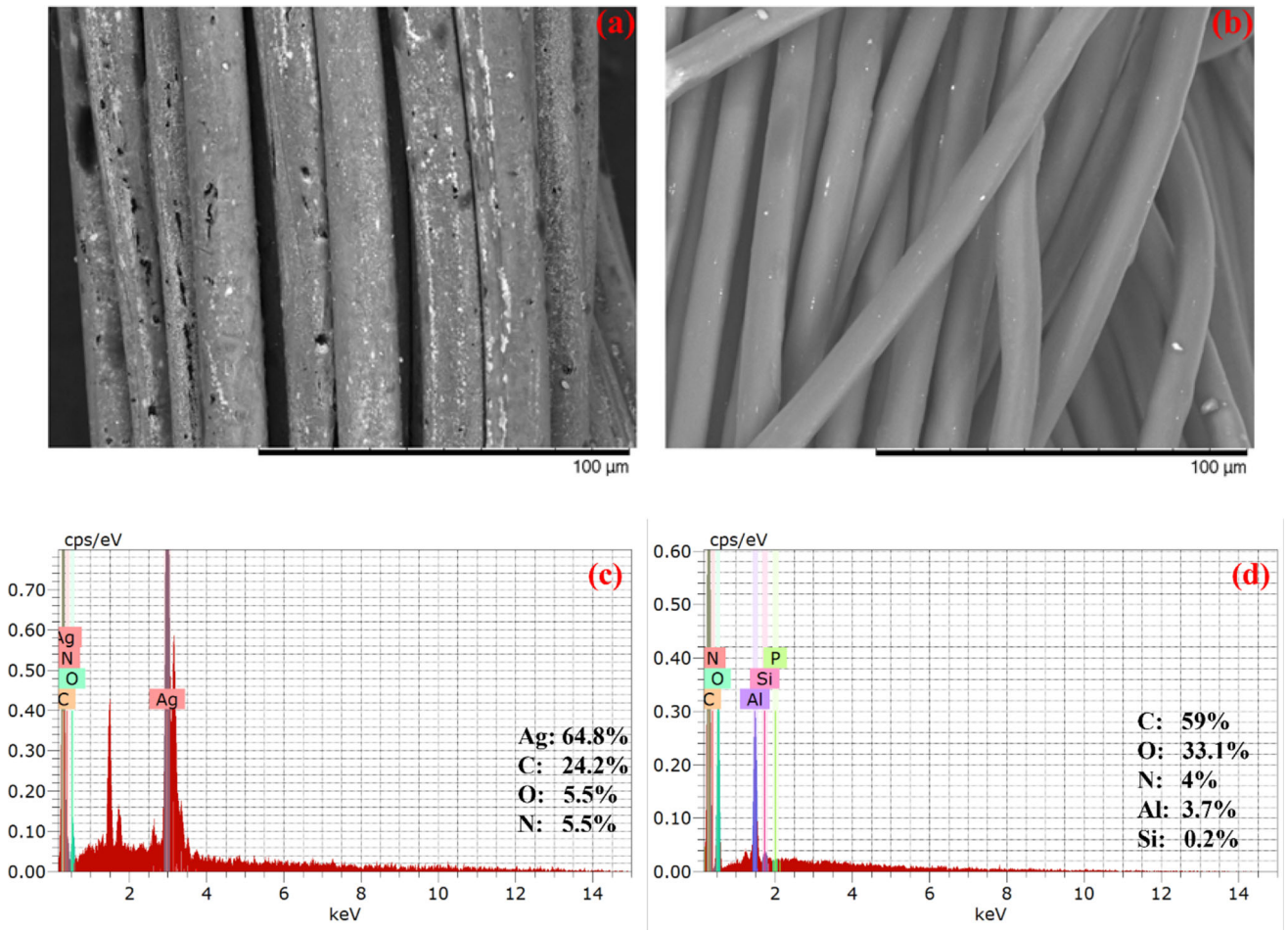

Figure 2 SEM micrograph of (**a**) Silver-Tech 150 conductive thread and (**b**) polyester Burmilon thread; EDX analysis of (**c**) Silver-Tech 150 and (**d**) polyester Burmilon threads with percent (%) composition of elements.

Resistance studies of the face mask sensor toward humidity monitoring

As a part of preliminary studies of the face mask sensor to demonstrate its behavior towards electrical parameters change over increasing frequencies, the variation of electrical resistance (real part of the electrical impedance) of the sensor was measured, at each RH level, as shown in Fig. 3. It can be concluded from the graph that the electrical resistance change is flatter at higher frequencies and the obtained results confirm the decreasing trend of electrical resistance of face mask sensor with the increase in frequencies suggesting high suitability of our prepared sensor for humidity monitoring [25–34].

Furthermore, the average sensitivity of the face mask sensor was calculated at each measurement frequency. For measurements at lower frequencies, 4 kHz, 8 kHz and 20 kHz, the average sensitivity of the sensor was found to be 27.75 kΩ/RH%, 10.20 kΩ/RH% and 4.79 kΩ/RH%, respectively. At 40 kHz, the sensitivity of the sensor was recorded as 2.2 kΩ/RH% which was decreased to 1.10 kΩ/RH% at 60 kHz. Further decrement in the sensitivity was observed as 0.32 kΩ/RH%, 0.20 kΩ/RH% and 0.12 kΩ/RH% at increased frequencies of 100 kHz, 150 kHz and 200 kHz, respectively. Figure 4a–h shows the decrease in the resistance values with the increase in the RH at different frequencies. However, the resistance values became flatter at higher frequencies as clearly shown in Fig. 4f–h. Furthermore, the linear performance of the sensor toward resistance change with the increasing % RH is shown in Fig. 5. The linear regression curve was plotted at different

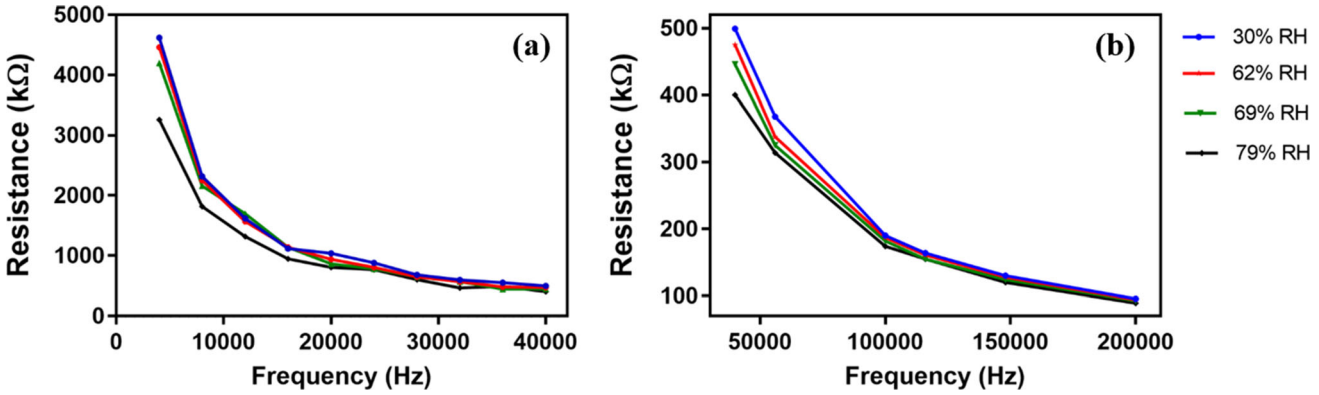

Figure 3 Resistance vs frequency change of the face mask sensor at different relative humidity levels: (**a**) in the lower frequency range (1 Hz to 40 kHz); (**b**) in the higher-frequency range (40 kHz to 200 kHz).

frequencies which showed a nominal decrement in resistance of fabricated face mask sensor with an increase in % RH. The percentage decrease in resistance between 30 and 79% relative humidity was 22.59%, 19.83%, 14.67% and 8.42% for 20 kHz, 40 kHz, 60 kHz and 100 kHz, respectively, which demonstrated that at lower measurement frequency, the humidity response signal of the face mask sensor was higher.

Real-time sensing of face mask sensor toward humidity detection

Three healthy male volunteers (subjects) were included in the real-time respiration monitoring study using the fabricated face mask sensor. All subjects signed the informed consent form, and before measurements, they were instructed to sit and rest for 5 min. The initial stage of the respiration monitoring was holding breath phase for 5 s, and after that, volunteers were instructed to breath normally. Subjects were sitting during the complete tests (approximately 80 s). Chemical impedance analyzer Hioki IM3590 was operated at low frequency in continuous sampling mode (90 samples per second). The reason for choosing low frequency for real-time testing is that around this frequency, the sensor showed more stable behavior, which is more suitable for portable devices and on-body in situ applications. Further, low-frequency range, allows us to create a low-cost readout electronic circuit where deviations of characteristics of filters, operational amplifiers or A/D convertors are generally avoided. The obtained results are shown in Figs. 6, 7, 8 and 9 for the following electrical parameters: impedance magnitude, phase angle, capacitance and resistance, respectively.

As shown in Figs. 6, 7, 8 and 9, all three parameters are sensitive to humidity changes caused by the respiration. However, we got very interesting results if compared the ratio of the peak-to-peak values (ends of exhalation and inhalation phase) of the one typical recorded cycle (marked with red rectangular shape in Figs. 6, 7, 8 and 9), as shown in Fig. 10. The sensitivity of electrical resistance ratio is the highest for all three subjects, followed by the impedance and capacitance, while the phase angle had the lowest peak-to-peak ratio.

Moreover, it can be noticed that there are some differences when absolute values of measured impedance, phase angle, capacitance and resistance are compared among three volunteers. This can be expected because of the following reasons. Primarily, volunteers had different breathing rate over the analyzed period of time (subject 1 had 13 inhalation/exhalation phases, while subject 2 had 16, and subject 3 had 21) causing different humidity levels in exhaled air. It can be expected that deeper and slower breathing will results in more humid exhaled air. However, this is not always true because a subject in calm position (or during sleeping) can have a very shallow and slow breathing. Therefore, the main reason for different resistance/capacitance values is different humidity of exhaled air. In addition to that, volunteers have different age and they also can have

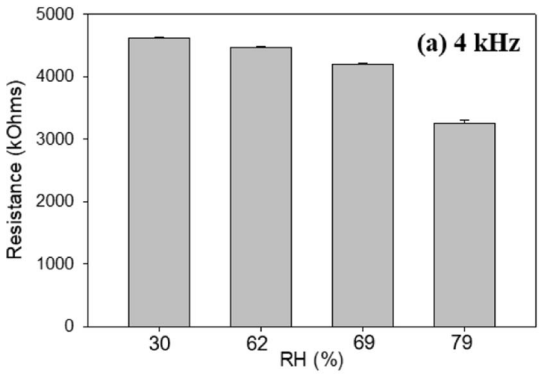
(a) 4 kHz
Resistance (kOhms)
5000
4000
3000
2000
1000
0
30
62
69
79
RH (%)

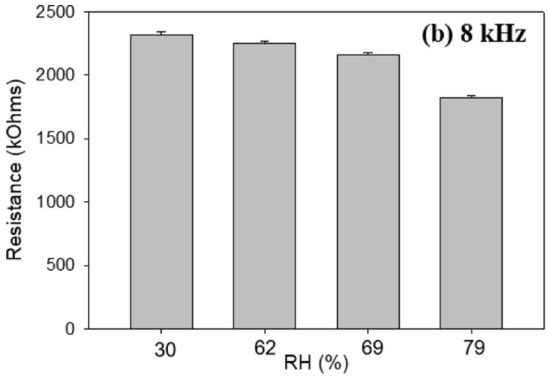
(b) 8 kHz
Resistance (kOhms)
2500
2000
1500
1000
500
0
30
62
69
79
RH (%)

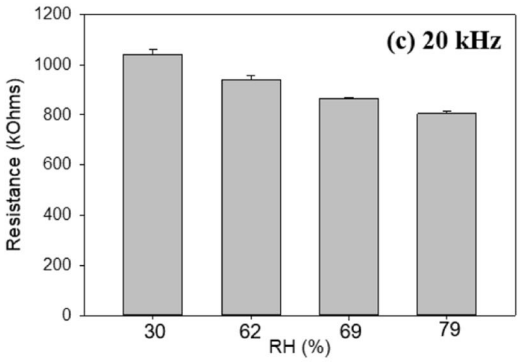
(c) 20 kHz
Resistance (kOhms)
1200
1000
800
600
400
200
0
30
62
69
79
RH (%)

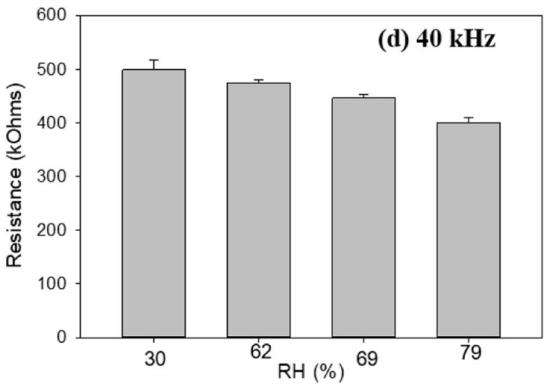
(d) 40 kHz
Resistance (kOhms)
600
500
400
300
200
100
0
30
62
69
79
RH (%)

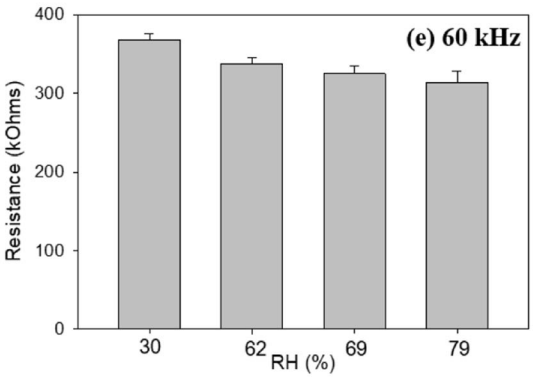
(e) 60 kHz
Resistance (kOhms)
400
300
200
100
0
30
62
69
79
RH (%)

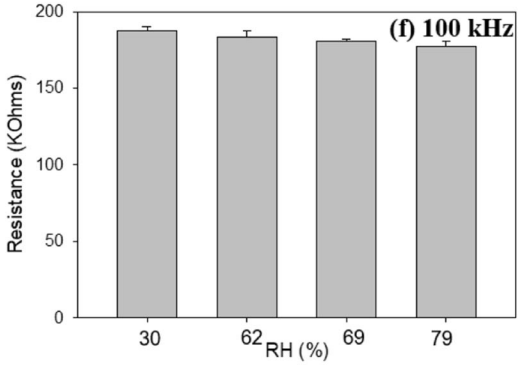
(f) 100 kHz
Resistance (KOhms)
200
150
100
50
0
30
62
69
79
RH (%)

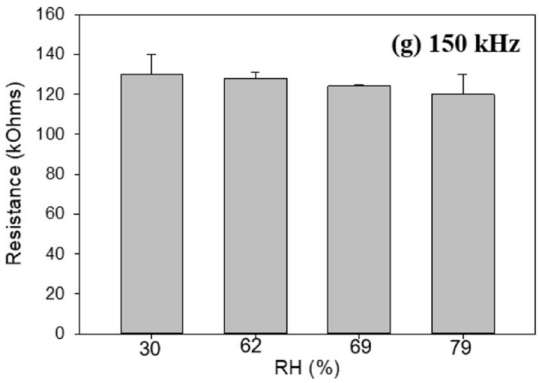
(g) 150 kHz
Resistance (kOhms)
160
140
120
100
80
60
40
20
0
30
62
69
79
RH (%)

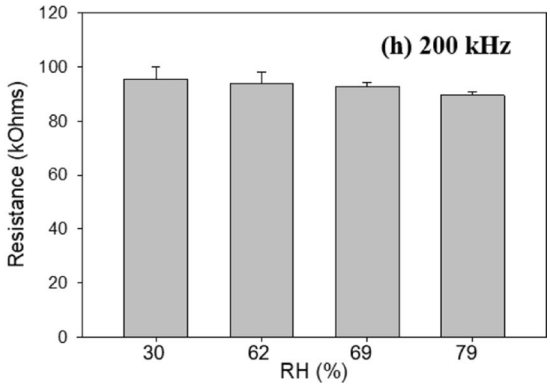
(h) 200 kHz
Resistance (kOhms)
120
100
80
60
40
20
0
30
62
69
79
RH (%)

◀**Figure 4** Change in resistance with the increase in relative humidity at different increasing frequencies.

wear mask with some differences in the shape of the mask (different bending) and position/distance of the sensor from the nose of the subject.

Response time can be determined as time required that signal reaches 90% of the steady state during the increase in the resistance during the respiration, while the recovery time can be determined as time required that signal drops 90% of the initial value during the decrease in the resistance. We chose obtained signals for Subject 3 because the fastest respiration was obtained, when compared to other two subjects. Response and recovery time can be obtained using graphical analysis as shown in Fig. 11 where obtained response time is 0.8 s, while the recovery time is about 1.5 s.

Finally, the calibration curve was obtained using the values shown Figs. 4 and 5, which enabled conversion of measured resistance to monitoring of RH changes during the respiration (Fig. 12). Bearing in mind that resistance decreased while RH increased, the same shape was obtained, but where electrical resistance as a function of time had maximum, relative humidity had minimum and vice versa.

Equivalent electrical circuit and analysis

Together with the Bode plots, the complex impedance spectroscopy is an alternative approach to discover the underlying sensing properties of the face mask sensor. As at low humidity levels, very few water molecules are adsorbed at sensor surface and

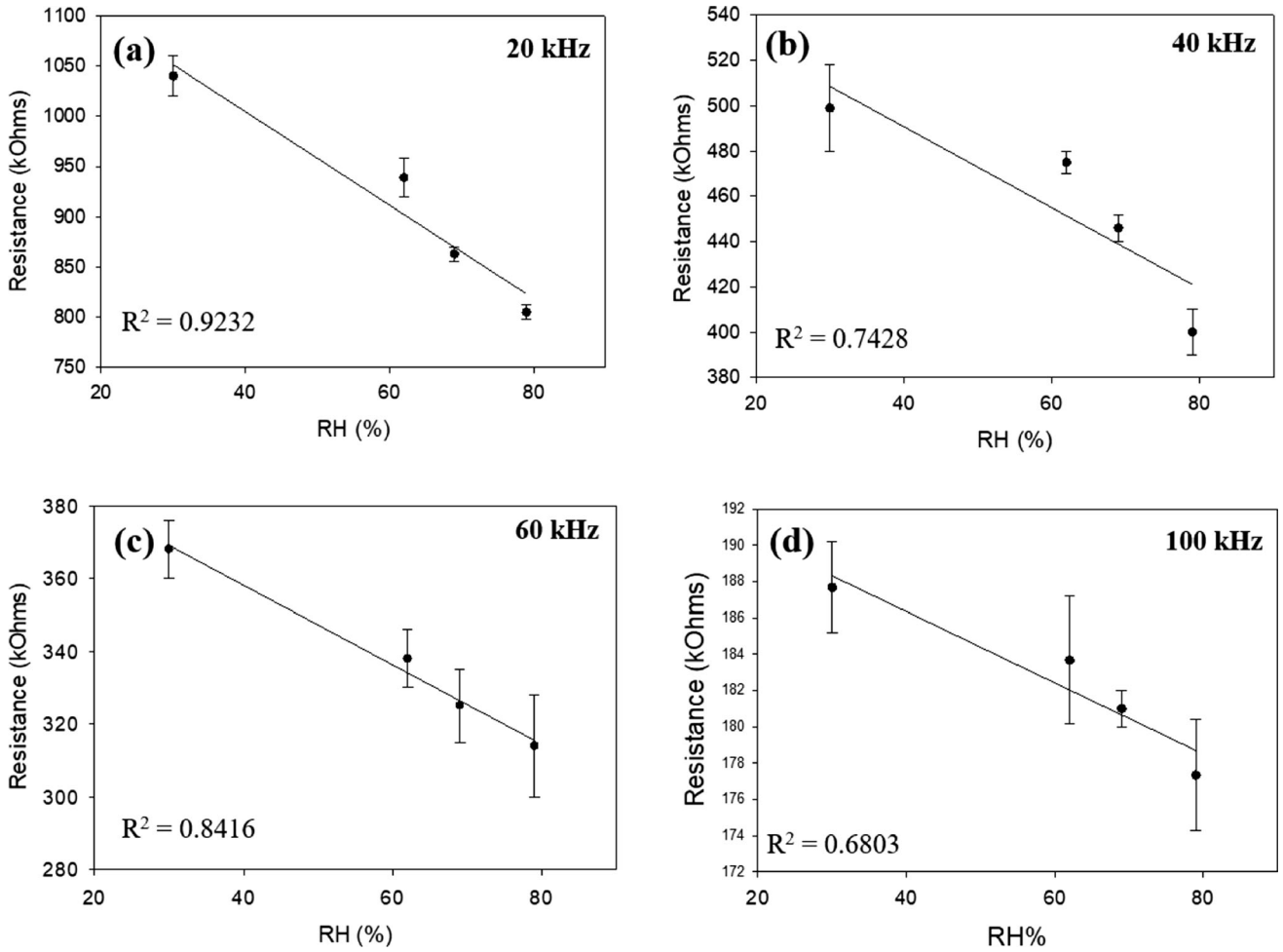

Figure 5 Linear plot showing change in resistance with the increase in relative humidity.

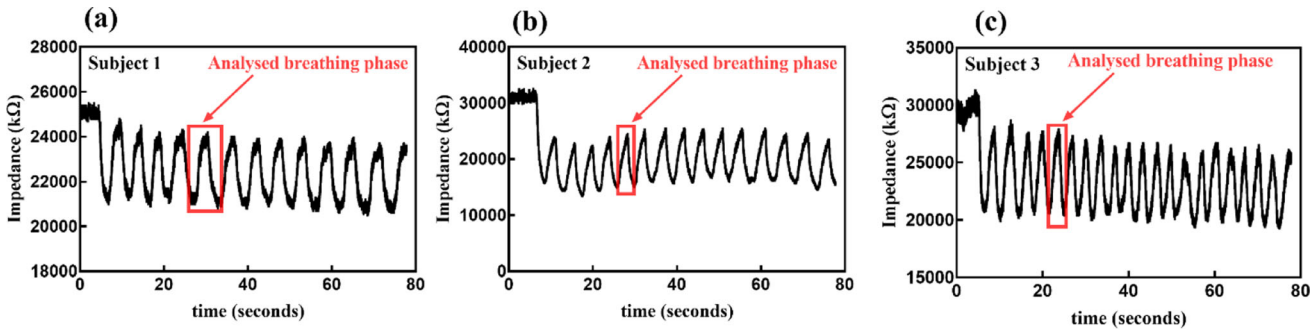

Figure 6 Measured values of impedance magnitude for volunteers during the normal respiration.

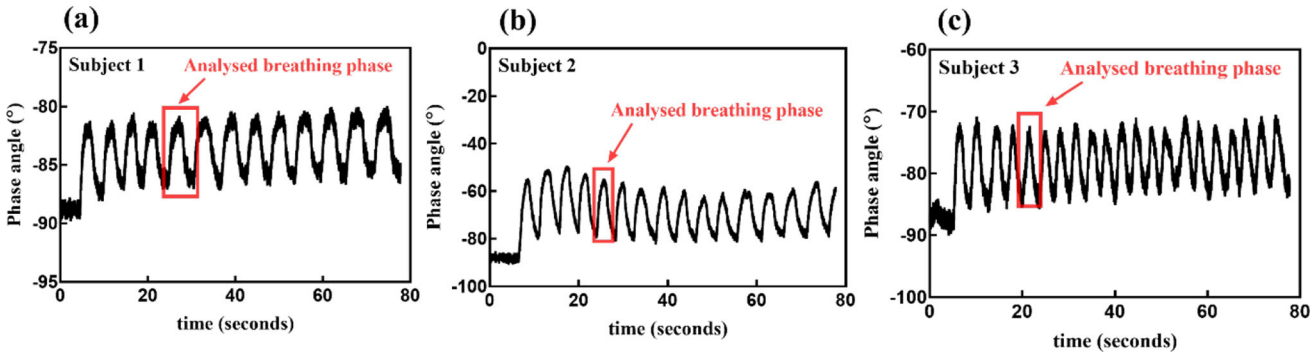

Figure 7 Measured values of impedance phase angle for volunteers during the normal respiration.

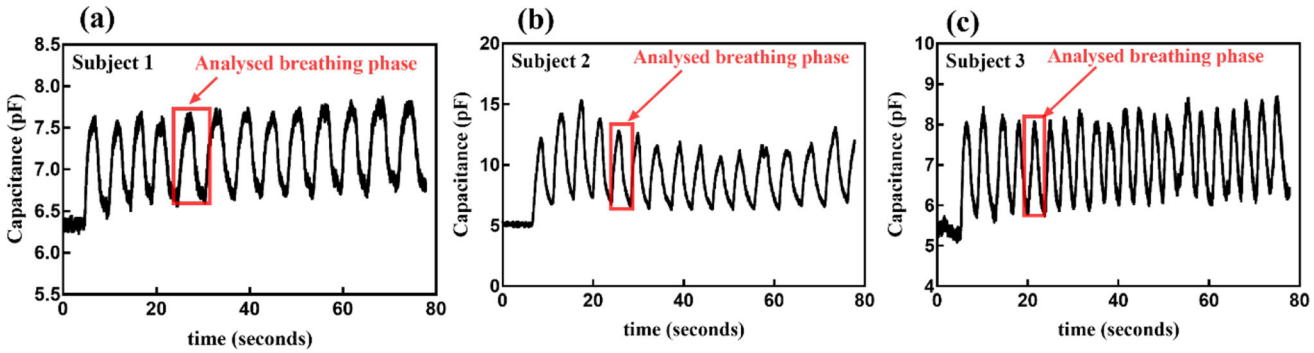

Figure 8 Measured values of capacitance for volunteers during the normal respiration.

the coverage of water on the film surface is not continuous [27] making the ion transport difficult. Thus, to analyze the electronic behavior of the face mask sensor, impedance spectroscopy was performed at increased relative humidity values of 68% and 79%. Figure 13 shows the Nyquist plots at the chosen %RH values, which were around the realistic values during the experiment as well as in real scenario. The increased humidity levels enhance the ionic conductivity or the electrolytic conduction within the moisture-sensitive threads as a result of which the characteristic semicircle in the Nyquist plot could be seen; however, it was not observed at lower humidity.

Based on the analysis of the fabricated structure as well as Nyquist plots, the equivalent electrical circuit

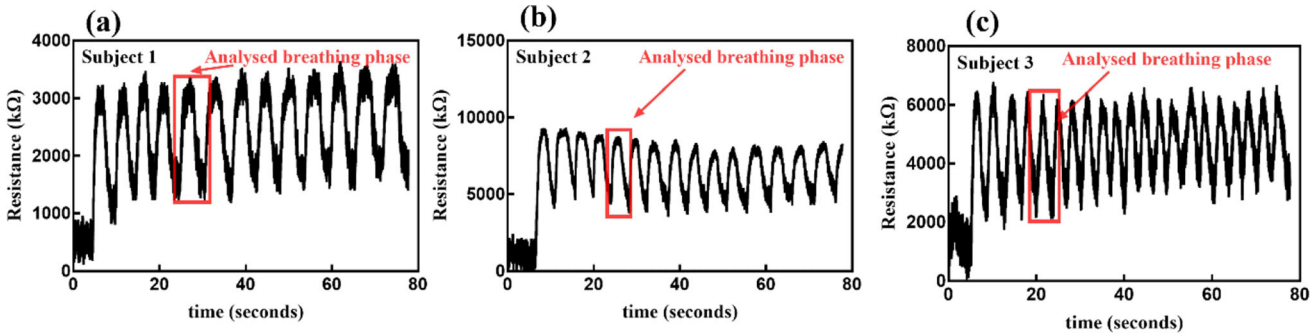

Figure 9 Measured values of resistance for volunteers during the normal respiration.

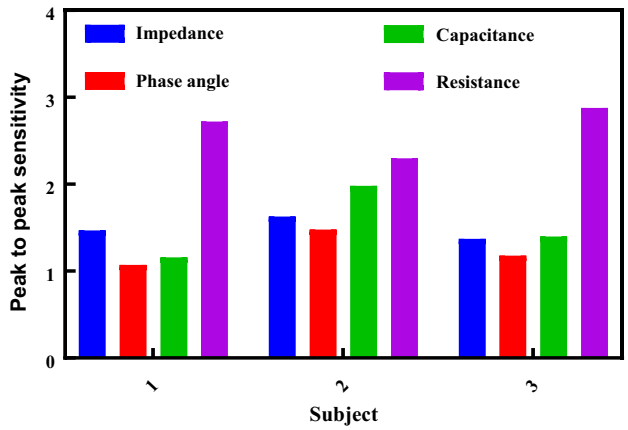

Figure 10 Peak-to-peak sensitivity of different parameters during the respiration of three volunteers.

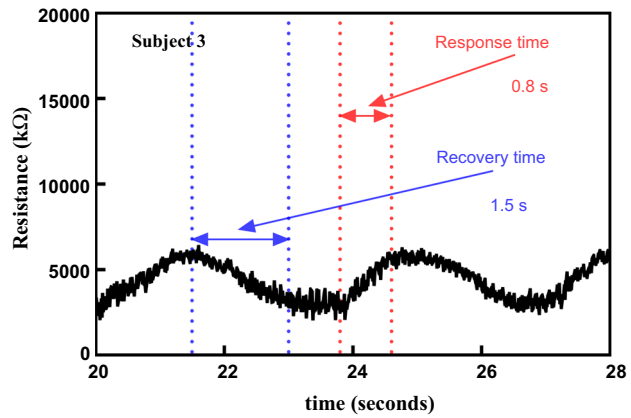

Figure 11 Determination of response and recovery times.

of the sensor is proposed. In general, it is a capacitive structure, but because of conductive path between electrodes when humidity is increased (during respiration), in parallel with capacitor C_1 should be placed a resistor R_1, as shown in Fig. 14.

Values of R1 and C1 are estimated using Fig. 13 for two relative humidity values (68% and 79%) at the low-frequency range (4 kHz). Obtained values are summarized in Table 2.

As shown in Table 2, there is a decrease in the resistive component with increasing humidity, while capacitance is increasing. These trends were expected as with increased RH, there should be increase in the capacitance because of increased dielectric constant of material between electrodes, as well as increase in the conductivity (decrease in the resistance). Another important observation is that rate of change for R1 is 5.37, while for C1 it is 1.20, which supports our assumption that range of variation of electrical resistance was higher than other sensing parameters.

Conclusion

In summary, for the first time, an electrical comparison of the responses of an embroidered face mask-based humidity sensor was recorded toward resistance, capacitance, impedance and phase angle change during respiration. The sensor was found highly sensitive toward moisture detection in the frequency range from 1 Hz to 200 kHz investigated between 30 and 79% RH levels and the results have

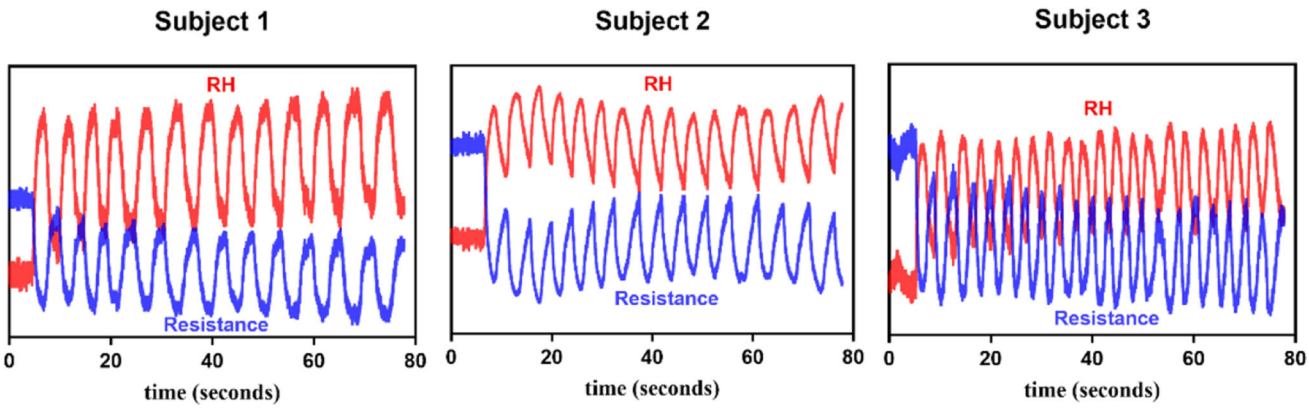

Figure 12 Changes of relative humidity and resistance during breathing of three subjects.

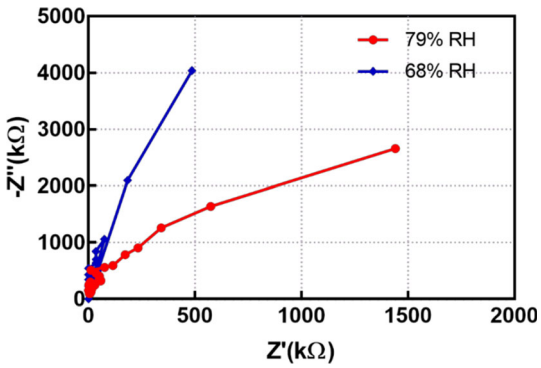

Figure 13 Nyquist plots of prepared face mask sensor obtained at higher humidity levels.

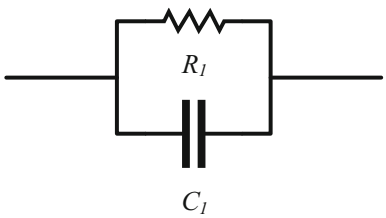

Figure 14 Proposed equivalent electrical circuit of the embroidered sensor.

Table 2 Estimated values of model parameters

Electrical parameter	68% RH	79% RH
R_1 (MΩ)	34.1	6.35
C_1 (pF)	9.71	11.61

been demonstrated using resistive type of sensing mechanism. We found that for this application, the electrical resistance demonstrated the highest peak-to-peak variation compering with other electrical parameters of IDE structure—impedance, phase angle or capacitance. The presented sensor prototype highlights the application of textile materials as a suitable and novel alternative to paper and hard polymer-based humidity sensors with high performance for various wearable e-textile applications.

Acknowledgements

This research was funded through the European Union's Horizon 2020 research and innovation program under Grant Agreement No. 854194.

Declarations

Conflict of interest The authors declare that they have no conflict of interest.

Supplementary Information: The online version contains supplementary material available at https://doi.org/10.1007/s10853-022-08135-2.

References

[1] Guntner AT, Abegg S, Konigstein K, Gerber PA, Trucksass AS, Pratsinis SE (2019) Breath sensors for health monitoring. ACS Sens 4:268–280

[2] Delipinar T, Shafique A, Gohar MS, Yapici MK (2021) Fabrication and materials integration of flexible humidity sensors for emerging applications. ACS Omega 6:8744–8753
[3] Wang Y, Huang J (2020) Recent advancements in flexible humidity sensors. J Semicond 41:2019–2021
[4] Duan Z, Jiang Y, Tai H (2021) Recent advances in humidity sensors for human body-related humidity detection. J Mater Chem C 9:14963–14980
[5] Rauf S, Vijjapu MT, Andrés MA, Gascón I, Roubeau O, Eddaoudi M, Salama KN (2020) Highly selective metal-organic framework textile humidity sensor. ACS Appl Mater Interfaces 12:29999–30006
[6] Wang W, Xiang C, Zhu Q, Zhong W, Li M, Yan K, Wang D (2018) Multistimulus responsive actuator with GO and carbon Nanotube/PDMS bilayer structure for flexible and smart devices. ACS Appl Mater Interfaces 10:27215–27223
[7] Su PG, Shiu WL, Tsai MS (2015) Flexible humidity sensor based on Au nanoparticles/graphene oxide/thiolated silica sol−gel film. Sens Actuators B 216:467–475
[8] Borini S, White R, Wei D, Astley M, Haque S, Spigone E, Harris N, Kivioja J, Ryhanen T (2013) Ultrafast graphene oxide humidity sensors. ACS Nano 7:11166–11173
[9] Duan Z, Jiang Y, Yan M, Wang S, Yuan Z, Zhao Q, Sun P, Xie G, Du X, Tai H (2019) Facile, flexible, cost-saving, and environment-friendly paper-based humidity sensor for multifunctional applications. ACS Appl Mater Interfaces 11:21840–21849
[10] Wang Y, Zhang L, Zhang Z, Sun P, Chen H (2020) High-sensitivity wearable and flexible humidity sensor based on graphene oxide/non-woven fabric for respiration monitoring. Langmuir 36:9443–9448
[11] Li B, Xiao G, Liu F, Qiao Y, Li CM, Lu Z (2018) Flexible humidity sensor based on silk fabric for human respiration monitoring. J Mater Chem C 6:4549–4554
[12] Weremczuk J, Tarapata G, Jachowicz R (2012) Humidity sensor printed on textile with use of ink-jet technology. Procedia Engineer 47:1366–1369
[13] Campos RK, Jin J, Rafael GH, Zhao M, Liao L, Simmons G, Chu S, Weaver SC, Chiu W, Cui Y (2020) Decontamination of SARS-CoV-2 and other RNA viruses from N95 level meltblown polypropylene fabric using heat under different humidities. ACS Nano 14:14017–14025
[14] Park SY, Lee JH (2021) Machine embroidered sensors for limb joint movement-monitoring smart clothing. Sensors 21:949–966
[15] Truong TT, Kim JS, Kim J (2022) Development of embroidery-type pressure sensor dependent on interdigitated capacitive method. Polymers 14:3446–3462
[16] Dizon AR, Orazem ME (2019) On the impedance response of interdigitated electrodes. Electrochim Acta 327:135000–135012
[17] Jin K, Zhao P, Fang W, Zhai Y, Hu S, Ma H, Li J (2020) An impedance sensor in detection of immunoglobulin G with interdigitated electrodes on flexible substrate. Appl Sci 10:4012–4020
[18] Sinha A, Stavrakis AK, Simic M, Stojanovic GM (2022) Polymer threads-based fully textile capacitive sensor embroidered on a protective face mask for humidity detection. ACS Omega 7:44928–44938
[19] Aeby X, Bourely J, Poulin A, Siqueira G, Nyström G, Briand D (2022) Printed humidity sensors from renewable and biodegradable materials. Adv Mater Technol 2201302
[20] Yang T, Yu YZ, Zhu LS, Wu X, Wang XH, Zhang J (2015) Fabrication of silver interdigitated electrodes on polyimide films viasurface modification and ion-exchange technique and its flexiblehumidity sensor application. Sensors Actuators B 208:327–333
[21] Thiwawong T, Onlaor K, Tunhoo B (2013) A humidity sensor based on silver nanoparticles thin film prepared by electrostatic spray deposition process. Adv Mater Sci Eng 2013:640428
[22] Li X, Zhuang Z, Qi D, Zhao C (2021) High sensitive and fast response humidity sensor based on polymer composite nanofibers for breath monitoring and non-contact sensing. Sensors Actuators B 330:129239–129249
[23] Chaloeipote G, Samarnwong J, Traiwatcharanon P, Kerdcharoen T, Wongchoosuk C (2021) High-performance resistive humidity sensor based on Ag nanoparticles decorated with graphene quantum dots. R Soc Open Sci 8:210407–210417
[24] Jang JH, Han JI (2017) Cylindrical relative humidity sensor based on poly-vinyl alcohol (PVA) for wearable computing devices with enhanced sensitivity. Sensors Actuators A 261:268–273
[25] Ma L, Wu R, Patil A, Zhu S, Meng Z, Meng H, Hou C, Zhang Y, Liu Q, Yu R, Wang J, Lin N, Liu XY (2019) Full-textile wireless flexible humidity sensor for human physiological monitoring. Adv Funct Mater 29:1–9
[26] Zhang D, Sun Y, Li P, Zhang Y (2016) Facile fabrication of MoS_2-modified SnO_2 hybrid nano-composite for ultrasensitive humidity sensing. ACS Appl Mater Interfaces 8:14142–14149
[27] Zhang D, Tong J, Xia B, Xue Q (2014) Ultrahigh performance humidity sensor based on layer-by layer self-assembly of graphene oxide/polyelectrolyte nanocomposite film. Sensors Actuators B 203:263–270
[28] McGhee JR, Sagu JS, Southee DJ, Evans PSA, Wijayantha KGU (2020) Printed, fully metal oxide, capacitive humidity

sensors using conductive indium tin oxide inks. ACS Appl Electron Mater 2:3593–3600

[29] Hong G, Choi S, Yoo DY, Oh T, Song Y, Yeon JH (2022) Moisture dependence of electrical resistivity in under-percolated cement-based composites with multi-walled carbon nanotubes. J Mater Res Technol 16:47–58

[30] Yukizaki H, Kawaguchi M, Egashira S, Hayashi Y (1998) Relationship between the electrical resistivity of enamel and the relative humidity. Connect Tissue Res 38:53–57

[31] Algie JE, Watt IC (1965) The effect of changes in the relative humidity on the electrical conductivity of wool fibers. Text Res J 35:922–929

[32] Zhang Y, Yu K, Jiang D, Zhu Z, Geng H, Luo L (2005) Zinc oxide nanorod and nanowire for humidity sensor. Appl Surf Sci 242:212–217

[33] Yao Z, Yang M (2006) A fast response resistance-type humidity sensor based on organic silicon containing cross-linked copolymer. Sens Actuators B 117:93–98

[34] Yoo KP, Lim LT, Nim NK, Lee MJ, Lee CJ, Park CW (2010) Novel resistive-type humidity sensor based on multiwall carbon nanotube/polyimide composite films. Sens Actuators B 145:120–125